SUPPLEMENTARY INFORMATION

Tet2-deficency in immune cells exacerbates tumor progression by increasing angiogenesis in a lung cancer model.

Yen T.M. Nguyen[1], Manabu Fujisawa[2], Tran B. Nguyen[2], Yasuhito Suehara[3], Tatsuhiro Sakamoto[2,3], Ryota Matsuoka[4], Yoshiaki Abe[1], Kota Fukumoto[3], Keiichiro Hattori[3], Masayuki Noguchi[4], Daisuke Matsubara[4,5], Shigeru Chiba[2,3], and Mamiko Sakata-Yanagimoto[2,3]

12 **SUPPLEMENTARY MATERIALS AND METHODS**

13 **Mice**

14 Polyinosinic: polycytidylic (pIpC) (Sigma, code# P0913) was intraperitoneally injected into
15 *Mx-Cre* x *Tet2*$^{flox/flox}$ and *Tet2*$^{flox/flox}$ mice at a dose 300μg/mouse every 2 days from day 2 after
16 birth with 3 doses in total. *Tet2* gene is disrupted in all hematopoietic cells in pIpC-treated *Mx-*
17 *Cre* x *Tet2*$^{flox/flox}$ mice. Female mice 6-8 weeks old were used for all experiments.

18

19 **Lung cancer cell lines**

20 LLC cells were expanded to enable injection into mice and for use in in vitro experiments. LLC
21 cells with at least 4 passages were used for experiments. LLC cells that had been passaged
22 more than 4 times were used for experiments.

23 The human lung cancer lines LC-Ad-1 and A549 were cultured in RPMI (Sigma-Aldrich,
24 code# r8758) plus 10% FBS and 1% PS. One week after thawing, these cell lines that had been
25 passaged more than 4 times were used for for S100A8/A9 stimulation experiments.

26

27 **Single cell suspensions from tumors**

28 Tumors were resected at day 18, or when the largest tumors reached 1000 mm^3. Tumors were
29 first minced with surgical scissors and the digested enzymatically for 30 minutes at 37° in 5
30 mL RPMI medium supplemented with 10% FCS and containing 0.75 mg/mL collagenase type
31 IV (Gibco, 17104-019) and 0.05 mg/mL DNase I (Worthington, code# DP100). Cells were
32 then passed through a 70 μm-strainer (Falcon, code# 352350) and then red blood cells were

33 lysed in ammonium-chloride-potassium buffer. Samples were centrifuged at 300 xg at 4ºC for
34 5 minutes, supernatants were discarded, and pellets were resuspended in PBS containing 2%
35 FCS (FACS buffer) to establish single-cell suspensions.

36

37 **Flow cytometric analysis**

38 Antibodies used were: anti-B220 (eBioscience, clone RA3-6B2, code# 25-0452-82) for B cells;
39 anti-Cd3 (eBioscience, clone 145-2C11, code# 17-0031-82), anti-Cd4 (eBiosciences, clone
40 GK1.5, code# 25-0042-82), and anti-Cd8 (BioLegend, clone 53-6.7, code# 100707) for T cells;
41 anti-Cd11b (BioLegend, clone M1/70, code# 101215), anti-Ly6c (BioLegend, clone HK1.4,
42 code# 128005), anti-Ly6g (BioLegend, clone RB6-8C5, code# 108411) for GMD and MMD;
43 anti F4/80 (eBiosciences, clone BM8, code# 17-4801-80) for TAMs; and anti-Emmprin
44 (BioLegend, clone OX-114, code# 123705), anti-Cd44 (eBiosciences, clone IM7, code# 11-
45 0441-81), and anti-Cd133 (eBiosciences, clone 13A4, code# 12-1331-80) for LLC cells. Cells
46 were then washed twice with FACS buffer, stained with 7AAD Viability Staining Solution,
47 and analyzed on FACS Aria II or III (BD Biosciences).

48

49 **RNA extraction, cDNA synthesis and quantitative RT-PCR**

50 Total RNAs were isolated from sorted or cultured cells using an RNeasy Mini Kit (Qiagen,
51 code# 74106), and RNA quality was determined by an Agilent 2100 Bioanalyzer using an
52 Agilent RNA 6000 Pico Chip (Agilent, code# 5067-1513). cDNAs were synthesized using
53 SuperScript™ III Reverse Transcriptase (10,000 units; Invitrogen, code# 18080-044). cDNA
54 quantity and quality were assessed using a Qubit 4 Fluorometer (Thermo Fisher Scientific) and
55 a Qubit™ dsDNA HS Assay Kit (Invitrogene, code# Q32851), respectively. Primers and

56 probes to determine expression levels of RNAs were TaqMan® Gene Expression Assays of
57 Thermo Fisher Scientific Il1b (Mm00434228_m1), S100a8 (Mm00496696_g1), S100a9
58 (Mm00656925_m1), Vegfa (Mm00437306_m1), and TaqMan Ribosomal RNA Control
59 Reagents for 18S ribosomal RNA (Thermo Fisher Scientific, code# 4308329). Quantitative
60 RT-PCR (qPCR) was performed on a 7500 Real-Time PCR system (Applied Biosystems) using
61 FastStart Universal Probe Master (Rox) (Roche, code# 38460200) according to manufacturer's
62 instructions. Expression of targeted transcripts was normalized to that of *Rn18s*.

63

64 **Whole transcriptome analysis (WTA)**

65 Cells were sorted directly in RLT buffer of the RNeasy Mini Kit (Cat# 74106) and then total
66 RNA was extracted.

67

68 **Reads alignment and differential expression analysis of WTA**

69 After quality control procedures, sequencing reads were mapped on the mm10 mouse reference
70 genome using the CLC Genomics Workbench ver.11 (Qiagen). The reads per kilobase of exon
71 model per million mapped reads (RPKM) value was calculated for each gene. The Differential
72 Expression for WTA tool was used to perform a statistical differential expression test between
73 *Tet2*$^{-/-}$ and *Tet2*$^{+/+}$ groups to identify DEGs between groups.

74

75 **Pathway and functional annotation analyses**

76 Gene set enrichment analysis (GSEA 4.1.0, https://www.gsea-msigdb.org/gsea/index.jsp) was
77 applied to identify significantly enriched pathways in each group. Gene sets from Molecular
78 Signatures Database (MSigDB 7.1) were used for analysis. Metascape

79 (https://metascape.org/gp/index.html#/main/step1) and DAVID Bioinformatics Resources 6.8
80 (https://david.ncifcrf.gov) were then applied for functional annotation of DEGs.
81
82 **Single cell RNA sequencing (scRNA-seq)**
83 Cd45^{+} immune cells were sorted from 1x10^{7} cells prepared from tumors from *Tet2*$^{+/+}$ or *Tet2*$^{-}$
84 $^{/-}$ mice using MACS Anti-APC MicroBeads (Miltenyi Biotec, code# 130-090-855) and APC
85 anti-mouse Cd45 antibody (Invitrogen, clone 104, code# 47-0454-80), according to
86 manufacturer's instruction. Library quality control and quantification were performed using a
87 2100 Bioanalyzer High Sensitivity DNA kit (Agilent, 5067-4626) and a KAPA Library
88 Quantification Kit (Kapa Biosystems, code# KK4824). Sequencing reads were mapped to the
89 mouse genome (build GRCm38) and demultiplexed using Cell Ranger pipelines (10x
90 Genomics, version 3.0.2).
91
92 **Data processing, integration and cell clustering**
93 Pre-processed data were further processed using R package *Seurat version 3.0 version* on
94 RStudio (version 1.4). Genes related to ribosomes were removed. Cells with fewer than 200
95 unique feature counts, those with unique feature counts greater than 5000, and those with the
96 number of mitochondrial genes > 5% were also removed. Data were normalized using the
97 "NormalizeData" function and highly variable features were extracted using the
98 "FindVariableFeatures" function. We then performed a linear transformation (scaling) and
99 principal component analysis (PCA) based on variable features using the "RunPCA" function.
100 Canonical correlation analysis (CCA) (27) was performed to identify shared sources of
101 variation across data of *Tet2*-deficient and WT Cd45^{+} cells using the "FindIntegrationAnchors"
102 function and integrate them using anchors using the "IntegrateData" function with canonical
103 correlation dimensions of 20.

104 Graph-based clustering was then performed using "FindNeighbors" and "FindClusters"
105 functions with the dimension of a reduction of 20, and resolution of 0.7. A non-linear
106 dimensional reduction Uniform Manifold Approximation and Projection (UMAP) technique
107 was used to visualize data using "RunUMAP" and "DimPlot" functions. Cell clusters were
108 annotated based on expression of canonical markers, including *Itgam*, *Gsr*, *Ly6g*, *Ly6c2* and
109 *Adgre1* for GMD, MMD and TAMs, *H2-Aa* and *H2-Eb1* for DCs, *Cd3e* for Lympho T cells
110 and *Cd79a* for Lympho B cells. The top 5 markers of each cluster were determined to identify
111 novel markers either highly or uniquely expressed in each cluster.
112
113 **DEG analysis**
114 "FindMarkers" or "FindAllMarkers" functions were used to detect DEGs in each subcluster
115 between *Tet2*-deficient and WT $Cd45^+$ cells, using the Wilcoxon Rank-Sum test and a
116 minimum log fold-change in gene expression between *Tet2*-deficient and WT cells of 0.25.
117 DEGs were defined as genes confirmed to show an adjusted p-value (based on the Bonferroni
118 correction) of < 0.05.
119
120 **Enzyme-linked immune sorbent assay (ELISA)**
121 To collect plasma, blood was taken from the superficial temporal vein into tubes containing 3
122 μL 0.5 mM EDTA, which were then centrifuged at 1000xg for 10 min at 4 °C. For cell culture,
123 supernatants were collected and then re-centrifuged at 300xg for 10 min at 4 °C. Supernatants
124 were transferred to new tubes and stored at -80 °C or assayed within one day.
125 S100a8, S100a9, Il1b, and Vegf were detected using mouse ELISA Kits for S100a8
126 (Abcam, code# ab213886), S100a9 (Abcam, code# ab213887), Il1b (Abcam, code# ab197742),
127 Vegf (Abcam, code# Ab100751) based on the manufacturer's protocol. A human VEGF

128 ELISA Kit (Abcam, code# 100662) was used to detect VEGF secreted from human lung cancer
129 lines.
130
131 **Proliferation assay**
132 A Cell Counting Kit (CCK)-8 assay (Dojindo, code# CK04-05) was used to measure
133 proliferation, based on the manufacturer's instructions. To do so, 1,000 LLC cells were seeded
134 into each well of 96-well flat plates (Corning, code# 3959) and then treated with a dilution
135 series of recombinant mouse S100a8/a9 heterodimer protein (R&D, 8916-S8-050) at 0, 0.001,
136 0.003, 0.01, 0.04, 0.156, 0.625, and 2.5 μg/ml, with 3 replicates for each concentration. At
137 indicated time points between 12 hours to 72 hours after treatment, 10 μL CCK-8 solution was
138 added to each well, cells were incubated at 37°C for 2 hours, and then assayed using a
139 Varioskan™ LUX multimode microplate reader (Thermo Fisher Scientific) at OD450.
140
141 **Treatment of cancer lines in vitro**
142 1 x10^5 LLC cells cultured in 12 well-plates were treated with or without 1 μg/ml recombinant
143 mouse S100a8/a9 heterodimer protein (R&D, code# 8916-S8-050). Supernatants were
144 collected after 24 hours to determine Vegf protein levels. In other experiments, 5 x10^5 human
145 cancer cells (LC-Ad-1 and A549) were similarly cultured, treated with recombinant human
146 S100A8/A9 heterodimer protein (R&D, code# 8226-S8-050), and assayed for VEGF
147 concentration.
148 To co-culture LLC cells with GMD cells, 5000 GMD were sorted from tumors of LLC-
149 injected *Tet2*$^{+/+}$ or *Tet2*$^{-/-}$ mice and then cultured in wells of 96-well plates in which LLC cells
150 had been previously cultured for 24 hours. Control wells contained only cultured LLC cells.
151 After 24 hours, supernatants from all samples were collected to determine Vegfa protein levels.
152 For Emmprin treatment, 1 hour after seeding GMD with LLC cells, anti-Emmprin antibody

153 (Cd147 monoclonal antibody functional grade; eBioscience, clone RL73, code# 16-1471-38)
154 or isotype control (rat IgG2a kappa isotype control functional grade; eBioscience, clone BR2a,
155 code# 16-4321-85) was added. After 24 more hours, supernatants were collected to determine
156 Vegfa protein levels.
157

158 **Immunohistochemical and immunofluorescence staining of tumor sections**

159 Portions of tumors resected from LLC-injected *Tet2*$^{+/+}$ and *Tet2*$^{-/-}$ mice were fixed in 10%
160 formalin for 24 hours at room temperature in 0.01 mol/L phosphate buffer (pH 7.2) and
161 embedded in paraffin. Sections were stained with hematoxylin and eosin (H&E) and
162 photographed using a Keyence BZ X710 microscope (Keyence Corporation, Osaka, Japan).
163 Other tumor portions were frozen in OCT compound (Sakura Finetek Japan Co.,code# 4583)
164 in hexane (Wako, code# 082-00426), chilled on dry ice, and then stored at -80ºC. OCT blocks
165 were sliced into 5 μm sections at -12ºC on a cryostat.

166 For immunohistochemistry staining of blood vessels, specimens were fixed with 4%
167 formaldehyde for 10 min at RT, and then endogenous peroxidase was blocked using fresh 3%
168 H_2O_2 for 10 min at RT. Sections were stained by anti-Cd31 antibody (BD Biosciences, code#
169 12-1331-80) (diluted 1:100) using a M.O.M. Immunodetection kit (Vector Laboratory, code#
170 BMK 22-02) for 30 min at RT and then incubated with the working solution of Biotinylated
171 Anti-rat IgG from the kit (diluted 1:100) for 30 min at RT. Sections were then incubated with
172 HRP-SA (Vector Laboratory, SA-5704-100) for 30 min at RT prior to addition of DAB (Dako,
173 code# K3468) to detect the signal. Finally, sections were washed 10 minutes in tap water,
174 counterstained with HE, dehydrated, coverslipped and then read on a Keyence (BZ-X710)
175 microscope. Each specimen was viewed in 5 fields at 20x magnification and Cd31-positive
176 areas were detected automatically using BZ-X Analyzer Software from Keyence (BZ-X710).

177 For immunofluorescent staining, sections were incubated with primary antibodies for 90
178 minutes at room temperature (RT). For Ly6g and Vegfa co-staining, anti-mouse-Ly6g (Thermo
179 Fisher Scientific, code# 13-5931-85) (1:10) and anti-mouse-Vegfa (Abcam, code# ab46154)
180 (1:100) antibodies were used. For Ly6g co-staining with S100a8, anti-S100a8 (Proteintech,
181 code# 15792-1-AP) (1:200) and anti-Ly6g (eBioscience, code# 11-5931-82) (1:50) antibodies
182 were used. For Ly6g co-staining with S100a9, anti-S100a9 (Proteintech, code# 14226-1-AP)
183 (1:100) and anti-Ly6g (eBioscience, code# 11-5931-82) (1:100) antibodies were used. As
184 secondary antibodies, goat anti-Rat IgG (H+L) Cross-Adsorbed Secondary Antibody, Alexa
185 Fluor 488 (Thermo Fisher Scientific, code# A-11006) (1:1000) was used for Ly6g (Thermo
186 Fisher Scientific, code# 13-5931-85) and goat anti-Rabbit IgG (H+L) Cross-Adsorbed
187 Secondary Antibody, Alexa Fluor 594 (Thermo Fisher Scientific, code# A-11072) (1:1000)
188 was used for Vegfa, S100a8 and S100a9 at RT for 30 minutes. After incubation with DAPI
189 (Vector laboratories, code# H-1200), stained samples were photographed using a Leica TCS
190 SP8 confocal laser scanning microscope (Leica Microsystems, Wetzlar, Germany).
191

192 **SUPPLEMENTARY NOTES**

193 **Pathway analysis reveals Il1b is a candidate upstream regulator of S100a8/S100a9**
194 **signaling**

195 To define factors that might regulate *S100a8/S100a9* in GMD cells, we performed Ingenuity
196 Pathway Analysis (IPA) analysis using DEGs ($p < 0.05$) from WTA of GMD. That analysis
197 revealed that Il1b signaling could be upstream of S100a8/S100a9 activity (Figure S6A). RNA-
198 seq data revealed that *Il1b* mRNA expression was significantly increased in *Tet2*-deficient
199 relative to WT GMD and MMD (Figure S6B). Gene set enrichment analysis (GSEA) also
200 showed that 6 pathways related to *Il1b* were enriched in *Tet2*-deficient compared to WT groups
201 (Figures S6C,D). Gene ontology analysis of DEGs from WTA of GMD, MMD and TAMs

202 revealed that the pathway "cellular response to IL-1" was among the top 10 common enriched
203 pathways, even from DEGs derived from scRNA-seq of $Cd45^{+}$ cells (Table S5, Figure S6E).
204 qPCR analysis confirmed that *Il1b* mRNA expression was higher in *Tet2*-deficient GMD than
205 in WT GMD (Figure S6F). Il1b protein levels in plasma were also higher in $Tet2^{-/-}$ relative to
206 $Tet2^{+/+}$ mice (Figure S6G).
207
208 **Prognostic impact for human lung cancer patients.**
209 Using the Gene Expression Profiling Interactive Analysis (GEPIA) database, we then
210 investigated the relationship between the genes encoding these mediators and their receptors
211 and the prognosis of lung cancer patients: both adenocarcinoma and squamous cell carcinoma.
212 In lung adenocarcinoma, patients showing high expression of S100A8, S100A9, EMMPRIN,
213 or VEGFA showed a poor overall survival and disease free survival, respectively (Figure S7A).
214 On the other hand, none of these factors served a predictive function in squamous cell lung
215 cancer (Figure S7B).
216
217
218 **SUPPLEMENTARY FIGURES**
219

Figure S1

(A)

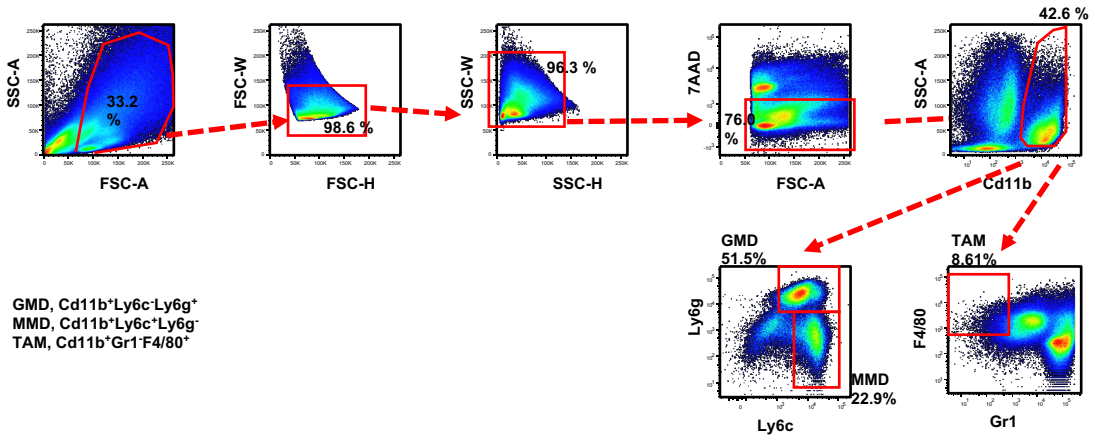

GMD, Cd11b^{+}Ly6c^{-}Ly6g^{+}
MMD, Cd11b^{+}Ly6c^{+}Ly6g^{-}
TAM, Cd11b^{+}Gr1^{-}F4/80^{+}

(B)

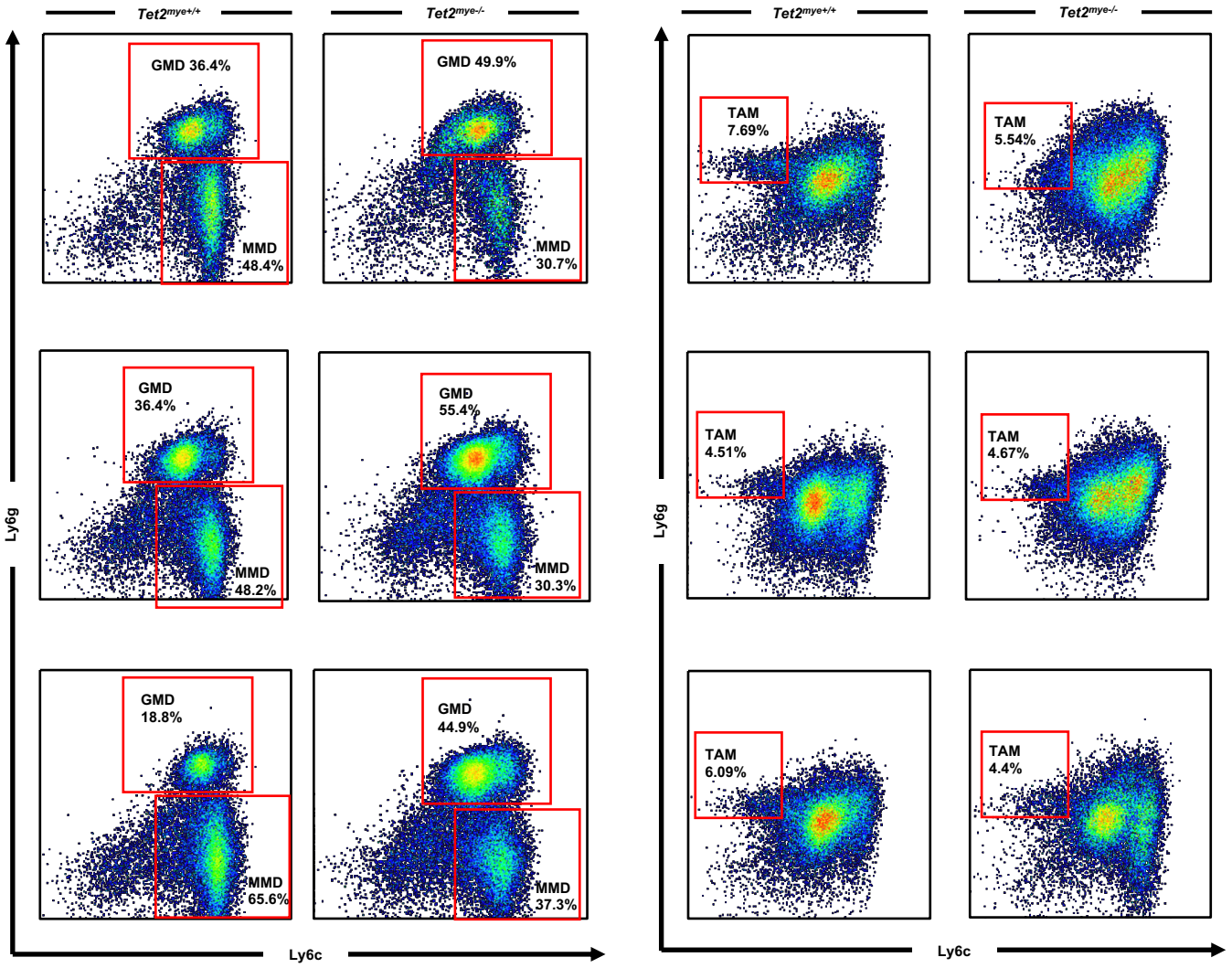

220 **Figure S1. *Tet2*-deficient immune cells enhance lung cancer progression in mice.**

221 A, Illustration of gating strategy used to isolate myeloid populations in tumors. GMD,

222 $CD11b^{+}Ly6C^{-}Ly6G^{+}$; MMD, $CD11b^{+}Ly6^{+}Ly6G^{-}$; TAMs, $CD11b^{+}Gr1^{-}F4/80^{+}$.

223 B, Representative flow cytometry plots: percentages of GMD, MMD and TAMs among

224 $Cd11b^{+}$ subsets from tumors. $Tet2^{mye+/+}$, n=3; $Tet2^{mye-/-}$, n=3.

225

226

Figure S2

(A)

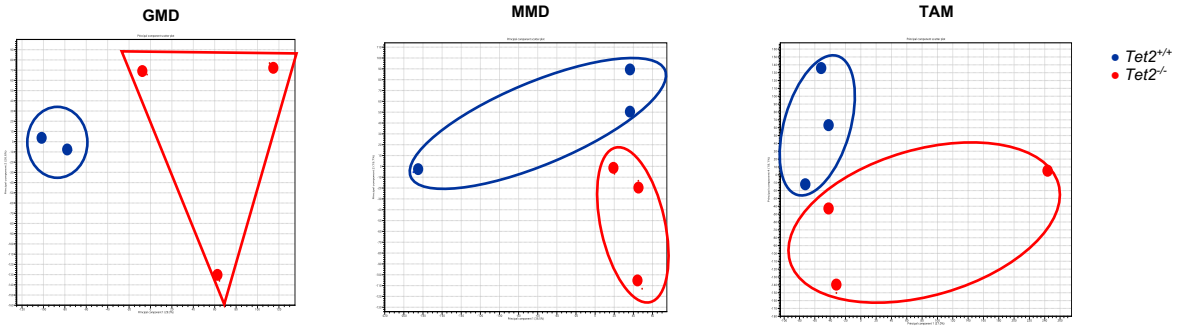
GMD
MMD
TAM
Tet2+/+
Tet2-/-

(B)

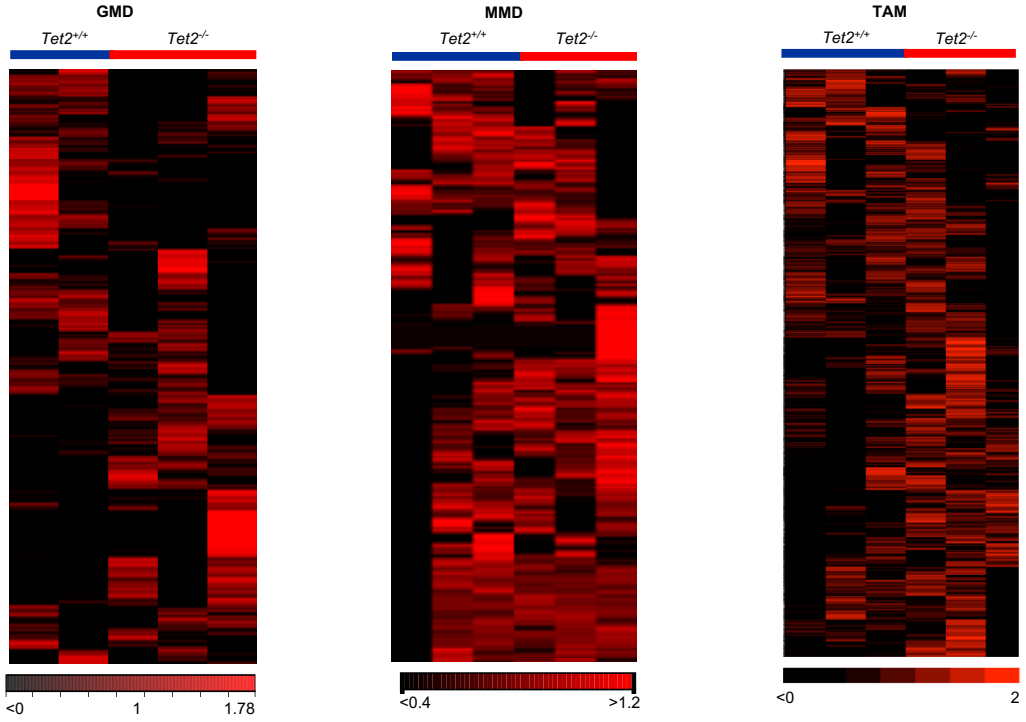
GMD
Tet2+/+
Tet2-/-
<0
1
1.78
MMD
Tet2+/+
Tet2-/-
<0.4
>1.2
TAM
Tet2+/+
Tet2-/-
<0
2

227 **Figure S2. Whole transcriptome analysis (WTA) reveals candidate mediators of LLC**
228 **growth expressed in *Tet2*-deficient myeloid cells.**
229 A, PCA plots for WTA of *Tet2*-deficient and WT GMD, MMD and TAMs.
230 B, Heatmaps of unsupervised clustering of genes differentially expressed in *Tet2*-deficient
231 relative to WT GMD, MMD and TAMs. Colors from black to bright red indicate gene
232 expression from low to high; color scale shows log2 expression values. *Tet2*-deficient and
233 WT groups were analyzed as 2 separate groups for each fraction.
234
235

Figure S3

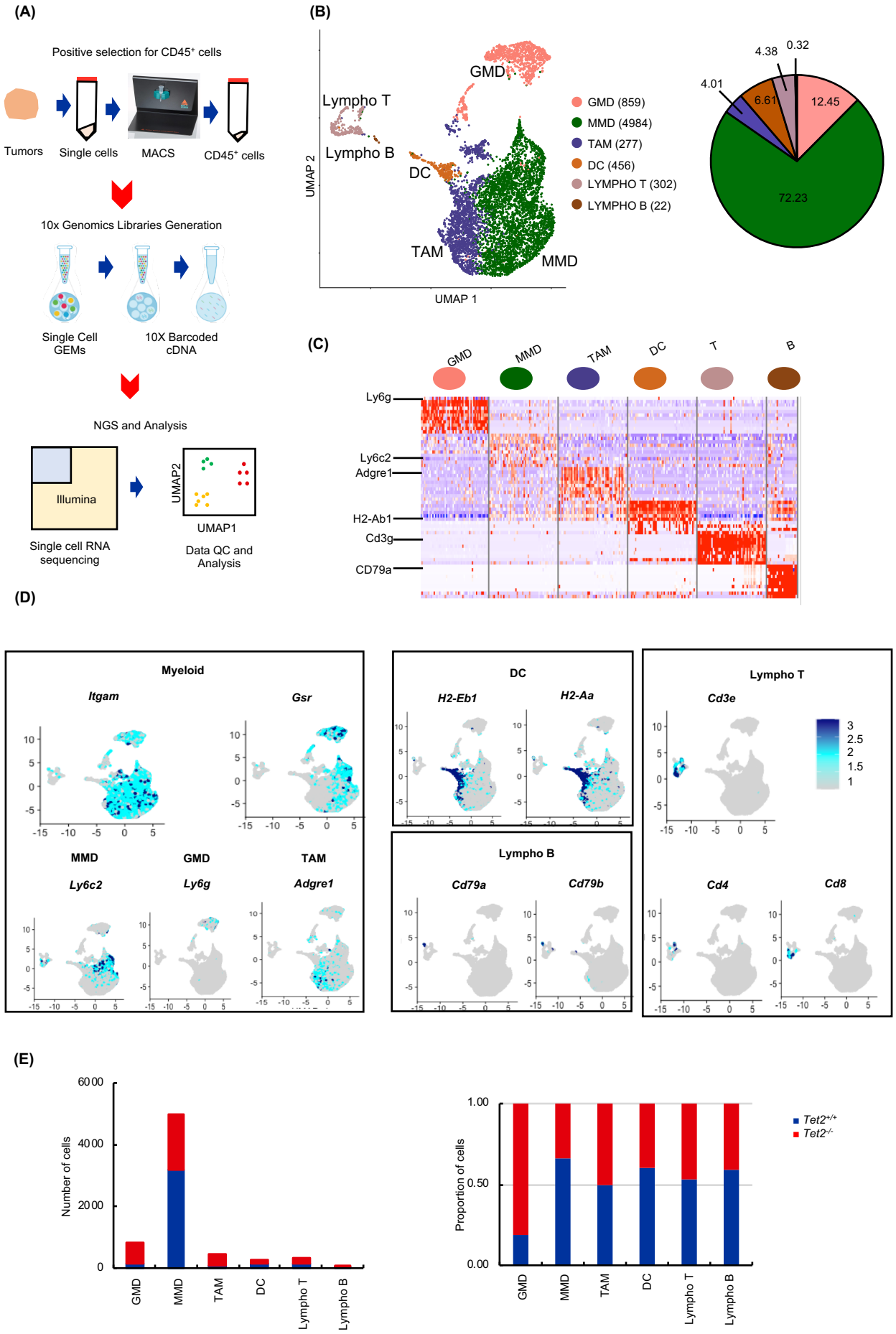
(A)
Positive selection for CD45⁺ cells
Tumors
Single cells
MACS
CD45⁺ cells
10x Genomics Libraries Generation
Single Cell GEMs
10X Barcoded cDNA
NGS and Analysis
Illumina
Single cell RNA sequencing
UMAP2
UMAP1
Data QC and Analysis
(B)
GMD
Lympho T
Lympho B
DC
TAM
MMD
UMAP 2
UMAP 1
GMD (859)
MMD (4984)
TAM (277)
DC (456)
LYMPHO T (302)
LYMPHO B (22)
4.38
0.32
4.01
6.61
12.45
72.23
(C)
GMD
MMD
TAM
DC
T
B
Ly6g
Ly6c2
Adgre1
H2-Ab1
Cd3g
CD79a
(D)
Myeloid
Itgam
Gsr
MMD
GMD
TAM
Ly6c2
Ly6g
Adgre1
DC
H2-Eb1
H2-Aa
Lympho B
Cd79a
Cd79b
Lympho T
Cd3e
Cd4
Cd8
(E)
Number of cells
GMD
MMD
TAM
DC
Lympho T
Lympho B
Proportion of cells
Tet2+/+
Tet2-/-

236 **Figure S3. Flowchart of single-cell transcriptome analysis to identify comprehensive**
237 **immune-cell profiles and candidate growth mediators in *Tet2*-deficient GMD.**
238 A, Overview of workflow for scRNA-seq performed in this study. MACS, Magnetic-activated
239 cell sorting; GEM, Gel Bead-in-Emulsion; NGS, next-generation sequencing; QC, Quality
240 Control.
241 B, A UMAP plot after integration of *Tet2*-deficient and WT $Cd45^+$ immune cells from tumors
242 (left). Six clusters corresponding to 6 cell types are labeled using different colors and the
243 number of cells in each cluster is shown. Pie graph shows the proportion of cells in each cluster
244 among total cells (right).
245 C, Heatmap of the top 10 conserved markers of each cell type.
246 D, Feature plots of common markers used to classify each cell type. Myeloid cells were divided
247 into MMD, GMD and TAMs by Itgam (Cd11b), Gsr (Gr1), Ly6c2, Ly6g and Adgre1 (F4/80).
248 DCs were identified by H2-Eb1 and H2-Aa (MHC-II markers), Lympho Ts by Cd3e, Cd4 and
249 Cd8a, and Lympho Bs by Cd79a and Cd79b.
250 E, Bar charts indicate cell number (left) and proportions (right) of 6 cell types.
251
252

Figure S4

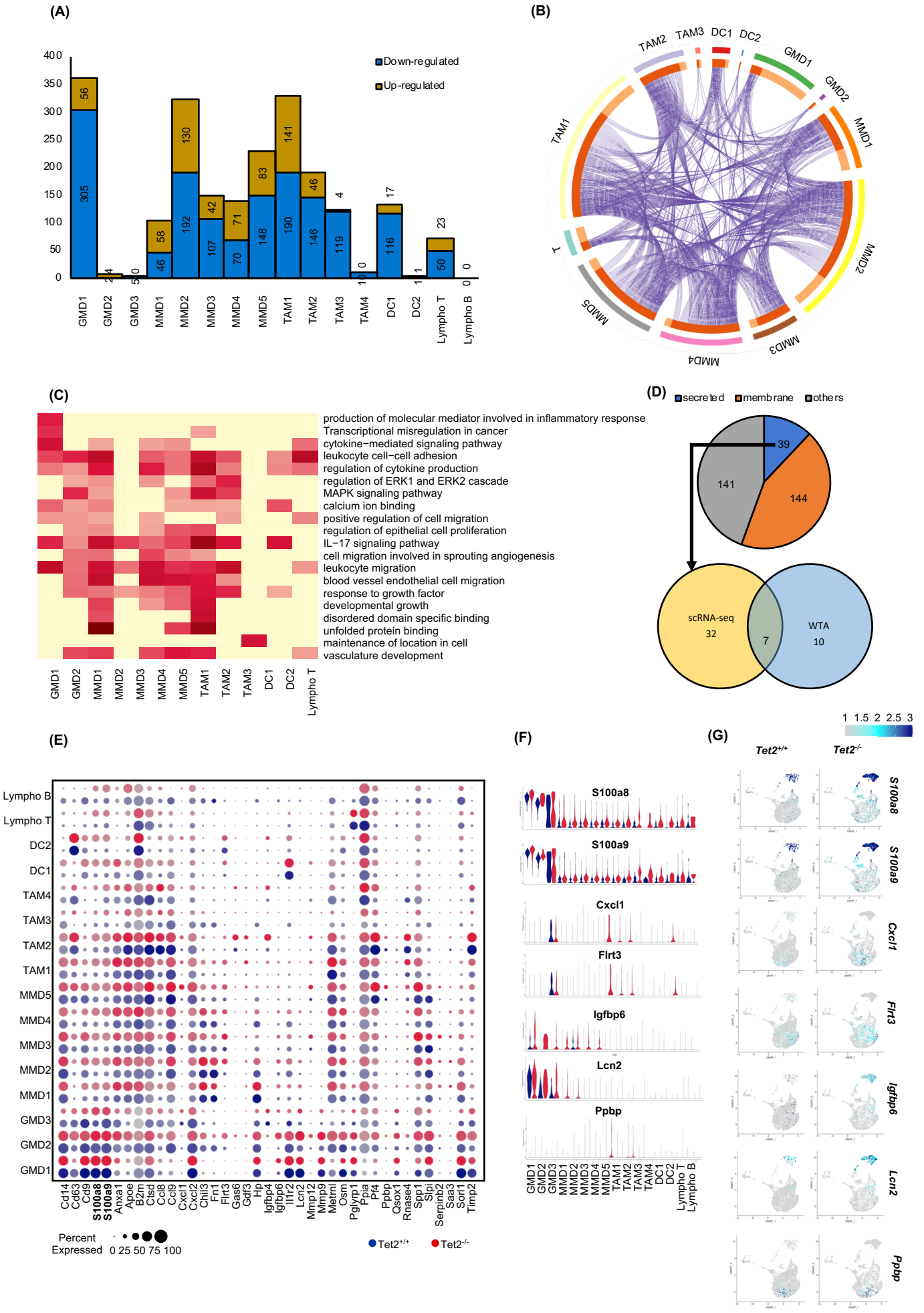
(A)
Down-regulated
Up-regulated
GMD1
GMD2
GMD3
MMD1
MMD2
MMD3
MMD4
MMD5
TAM1
TAM2
TAM3
TAM4
DC1
DC2
Lympho T
Lympho B
(B)
TAM2
TAM3
DC1
DC2
GMD1
GMD2
MMD1
MMD2
MMD3
MMD4
MMD5
T
TAM1
(C)
production of molecular mediator involved in inflammatory response
Transcriptional misregulation in cancer
cytokine−mediated signaling pathway
leukocyte cell−cell adhesion
regulation of cytokine production
regulation of ERK1 and ERK2 cascade
MAPK signaling pathway
calcium ion binding
positive regulation of cell migration
regulation of epithelial cell proliferation
IL−17 signaling pathway
cell migration involved in sprouting angiogenesis
leukocyte migration
blood vessel endothelial cell migration
response to growth factor
developmental growth
disordered domain specific binding
unfolded protein binding
maintenance of location in cell
vasculature development
(D)
secreted
membrane
others
39
141
144
scRNA-seq
32
7
WTA
10
(E)
Percent Expressed
0 25 50 75 100
Tet2+/+
Tet2-/-
(F)
S100a8
S100a9
Cxcl1
Flrt3
Igfbp6
Lcn2
Ppbp
(G)
Tet2+/+
Tet2-/-
S100a8
S100a9
Cxcl1
Flrt3
Igfbp6
Lcn2
Ppbp

253 **Figure S4. Single-cell transcriptome analysis revealed comprehensive immune cell**
254 **profiles and identified candidate mediators in *Tet2*-deficient GMD.**
255 A, The number of DEGs in the indicated 16 clusters from *Tet2*-deficient immune cells relative
256 to WT. Cut-off, adjusted P value < 0.05.
257 B, A circos plot from Metascape analysis indicates upregulated genes overlapping among the
258 13 clusters shown in (A). (GMD3, TAM4 and Lympho B were excluded due to lack of
259 upregulated genes.)
260 C, Metascape analysis showing the top 20 enrichment pathways of the 13 clusters described in
261 (B). Cut-off, adjusted P value < 0.01.
262 D, Pie graph (top) including 324 up-regulated markers from the 13 clusters described in (B).
263 David analysis was performed to narrow them to 39 genes that encoded secreted proteins (blue),
264 144 that encoded membrane proteins (orange), and 141 others (grey). The Venn diagram
265 (bottom) shows the inter-relationship between scRNA-seq and WTA data from GMD, MMD
266 and TAMs for genes encoding secreted proteins, with 7 shared genes, and 32 and 17 specific
267 to either scRNA-seq and WTA, respectively.
268 E, A dot plot of 39 genes encoding secreted proteins in scRNA-seq. Cut-off, adjusted P value
269 < 0.05. Dot size and color indicate the percentage of cells and expression level in each
270 subcluster, respectively.
271 F, G, Wrap Plots (F) and Feature Plots (G) of 7 genes from (D) shared by scRNA-seq and
272 WTA.
273
274

Figure S5

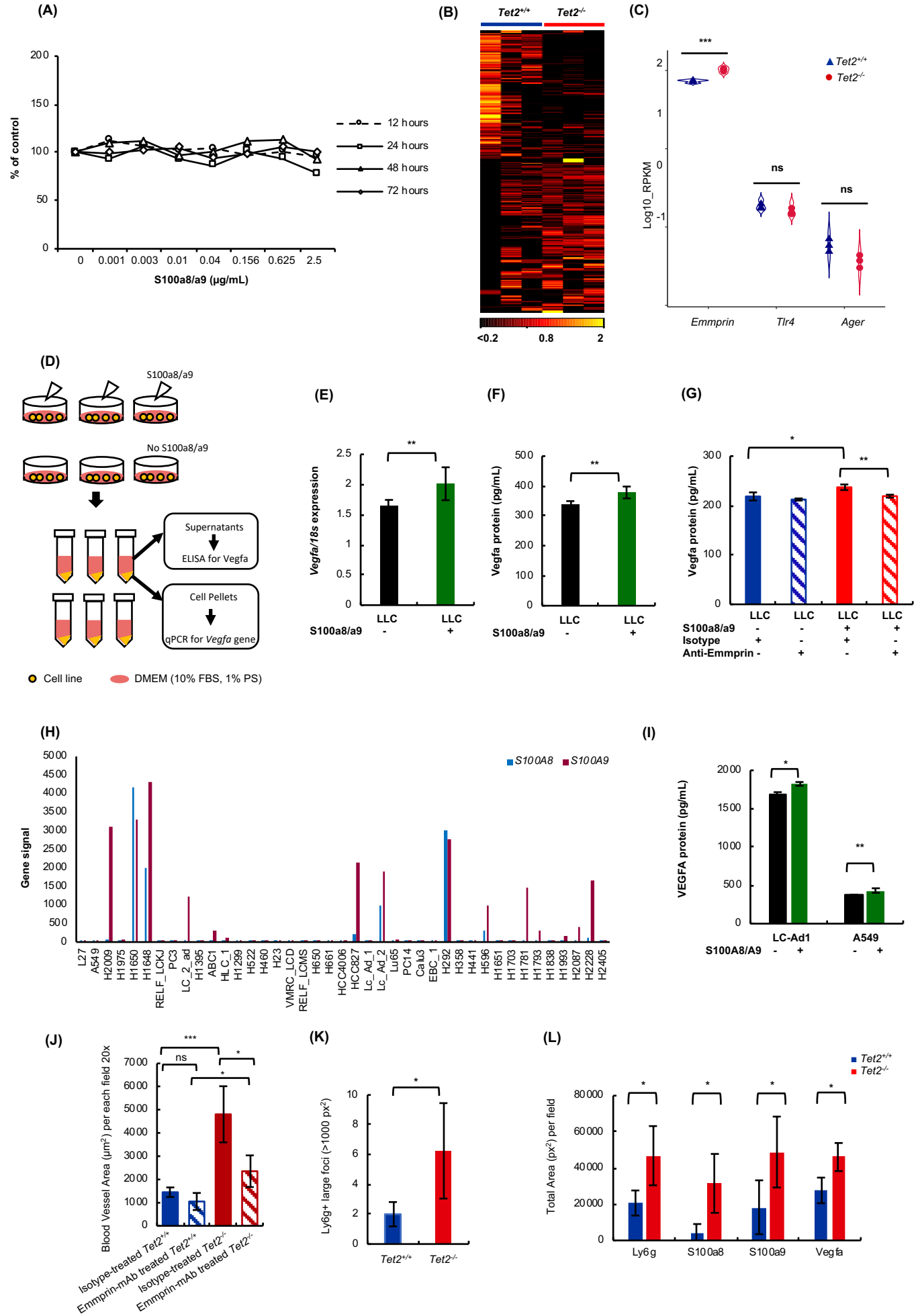
(A)
% of control
S100a8/a9 (µg/mL)
12 hours
24 hours
48 hours
72 hours
(B)
Tet2+/+
Tet2-/-
<0.2
0.8
2
(C)
Log10_RPKM
Tet2+/+
Tet2-/-
***
ns
ns
Emmprin
Tlr4
Ager
(D)
S100a8/a9
No S100a8/a9
Supernatants
ELISA for Vegfa
Cell Pellets
qPCR for Vegfa gene
Cell line
DMEM (10% FBS, 1% PS)
(E)
Vegfa/18s expression
S100a8/a9
(F)
Vegfa protein (pg/mL)
S100a8/a9
(G)
Vegfa protein (pg/mL)
S100a8/a9
Isotype
Anti-Emmprin
(H)
Gene signal
S100A8
S100A9
(I)
VEGFA protein (pg/mL)
LC-Ad1
A549
S100A8/A9
(J)
Blood Vessel Area (µm²) per each field 20x
Isotype-treated Tet2+/+
Emmprin-mAb treated Tet2+/+
Isotype-treated Tet2-/-
Emmprin-mAb treated Tet2-/-
(K)
Ly6g+ large foci (>1000 px²)
Tet2+/+
Tet2-/-
(L)
Total Area (px²) per field
Tet2+/+
Tet2-/-
Ly6g
S100a8
S100a9
Vegfa

275 **Figure S5. Vegfa protein secretions are stimulated by S100a/S100a9 in both mouse and**
276 **human lung cancer cells.**
277 A, Growth of LLC cells treated in vitro with S100a8/a9 protein. 1000 LLC cells were
278 stimulated at indicated concentrations of S100a8/a9 for 12, 24, 48, or 72 hours.
279 B, Heatmap of unsupervised clustering of genes differentially expressed in LLC cells sorted
280 from tumors in *Tet2*$^{-/-}$ mice versus those from tumors in *Tet2*$^{+/+}$ mice. Colors ranging from
281 black, to red to yellow indicates different gene expression from low to high. The color scale
282 below indicates log2 expression values. LLC cells in tumors from *Tet2*$^{-/-}$ and *Tet2*$^{+/+}$ mice were
283 analyzed as 2 separate groups.
284 C, Expression of *Bsg, Tlr4* and *Ager*, which encode Emmprin, Tlr4 and RAGE, respectively,
285 which reportedly serve as S100a8 and S100a9 receptors. RPKM were calculated from WTA
286 of indicated tumor-derived LLC cells.
287 D, Experimental schema showing strategy to measure Vegfa protein in supernatants of LLCs
288 treated with S100a8/a9 protein.
289 E, *Vegfa* expression normalized to *Rn18s* in LLC cells stimulated in vitro with S100a8/a9
290 protein. For replicates of each group, n = 4.
291 F, Vegfa protein levels in supernatants of LLC cells described in (E), as detected by ELISA.
292 For replicates of each group, n = 4.
293 G, Vegfa protein levels in supernatants of LLC cells stimulated in vitro with S100a8/a9 protein
294 under the treatment of anti-Emmprin antibody or isotype, as detected by ELISA. For replicates
295 of each group, n = 3.
296 H, The signal of *S100A8* and *S100A9* from microarray data of 41 human cell lines.
297 I, VEGF protein levels in supernatants of LC-Ad-1 or A549 cells treated in vitro with
298 S100a8/a9 protein, as detected by ELISA. For replicates of each group, n = 4.

299 J, Blood vessel area per each field at 20x magnification (5 random fields of view per sample)
300 in tumor sections from *Tet2*$^{-/-}$ and *Tet2*$^{+/+}$ mice treated with either anti-Emmprin antibody or
301 isotype control. Isotype-treated *Tet2*$^{+/+}$ (n=3), Isotype-treated *Tet2*$^{-/-}$ (n=5), Emmprin-mAb
302 treated *Tet2*$^{+/+}$ (n=3) and Emmprin-mAb treated *Tet2*$^{-/-}$ (n=3).
303 K, The number of Ly6g^{+} foci, whose area are larger than 1000 μm^{2} per each field at 20x
304 magnification in tumor sections from *Tet2*$^{-/-}$ (n=4) and *Tet2*$^{+/+}$ (n=4) mice.
305 L, Positive area (μm^{2}) of Ly6g, S100a8, S100a9 and Vegfa per field at 20x magnification in
306 tumor sections from *Tet2*$^{-/-}$ (n=4) and *Tet2*$^{+/+}$ (n=4) mice.
307
308

Figure S6

(A)

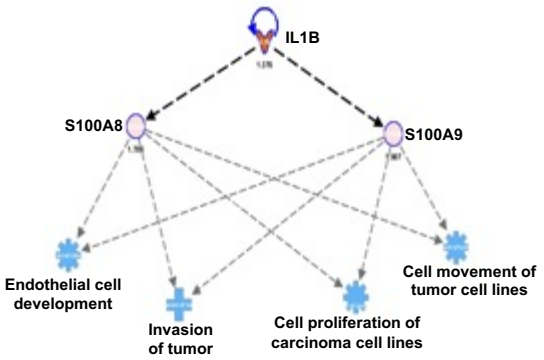

(B)

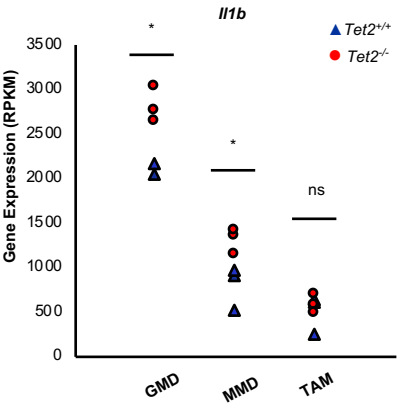

(C)

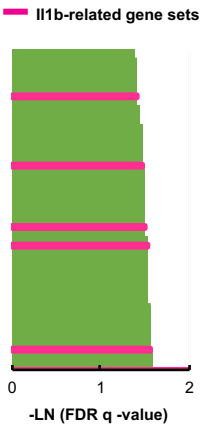

(D)

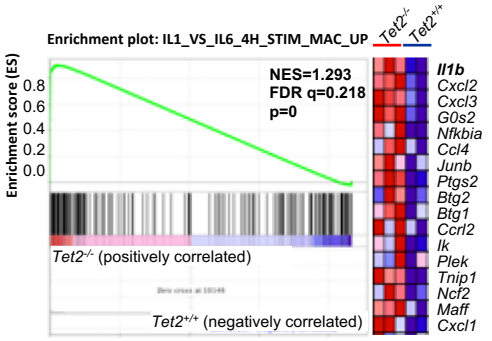

(E)

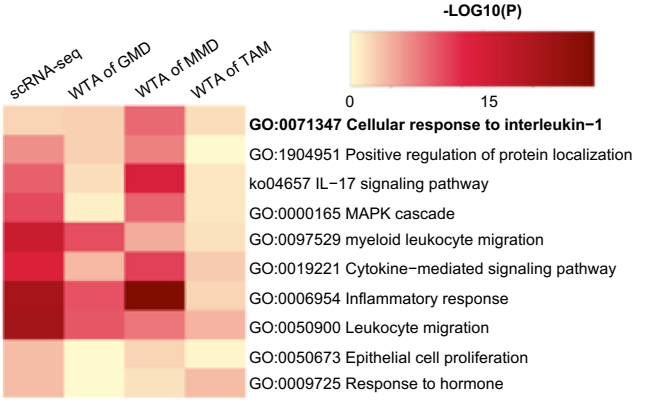

(F)

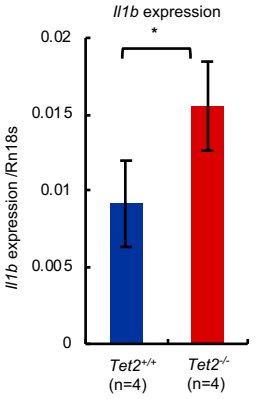

(G)

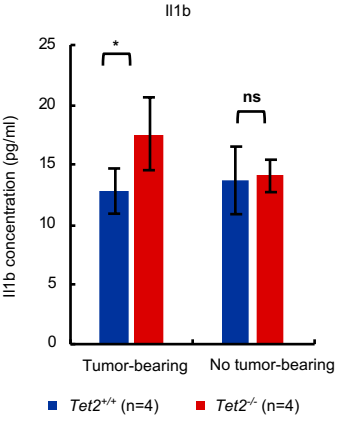

309 **Figure S6. Pathway analysis revealing Il1b as a candidate regulator of S100a8/S100a9**
310 **signaling.**

311 A, Ingenuity pathway analysis (IPA) of DEGs in GMD (cut-off, $p < 0.05$) to assess signaling
312 upstream and downstream of S100a8 and S100a9. Il1b was identified as a candidate upstream
313 factor. Four predicted downstream pathways are shown in blue.

314 B, Reads Per Kilobase of transcript, per Million mapped reads (RPKM) values of *Il1b* from
315 WTA data in either *Tet2*-deficient or WT GMD, MMD and TAMs.

316 C, Gene sets enriched in *Tet2*-deficient relative to WT groups for WTA data from GMD. Pink
317 bars; Il1b-related gene sets (cut-off; FDR $q < 0.25$, nominal $p < 0.05$).

318 D, Enrichment plot and heatmap of one enriched pathway related to *Il1b*, namely, the
319 IL1_VS_IL6_4H_STIM_MAC_UP pathway, using WTA data from GMD.

320 E, Metascape analysis revealing the top 10 enrichment pathways as determined from
321 upregulated gene sets of scRNA-seq data and WTA of GMD, MMD, and TAMs.

322 F, *Il1b* mRNA expression normalized to *Rn18s* in GMD sorted from tumors from *Tet2*$^{-/-}$ (n =
323 3) and *Tet2*$^{+/+}$ (n = 4) mice.

324 G, Il1b protein levels in plasma of either tumor-bearing or non-tumor-bearing mice, based on
325 ELISA. Each group, n = 4.

326

327

Figure S7

(A)

Lung adenocarcinoma

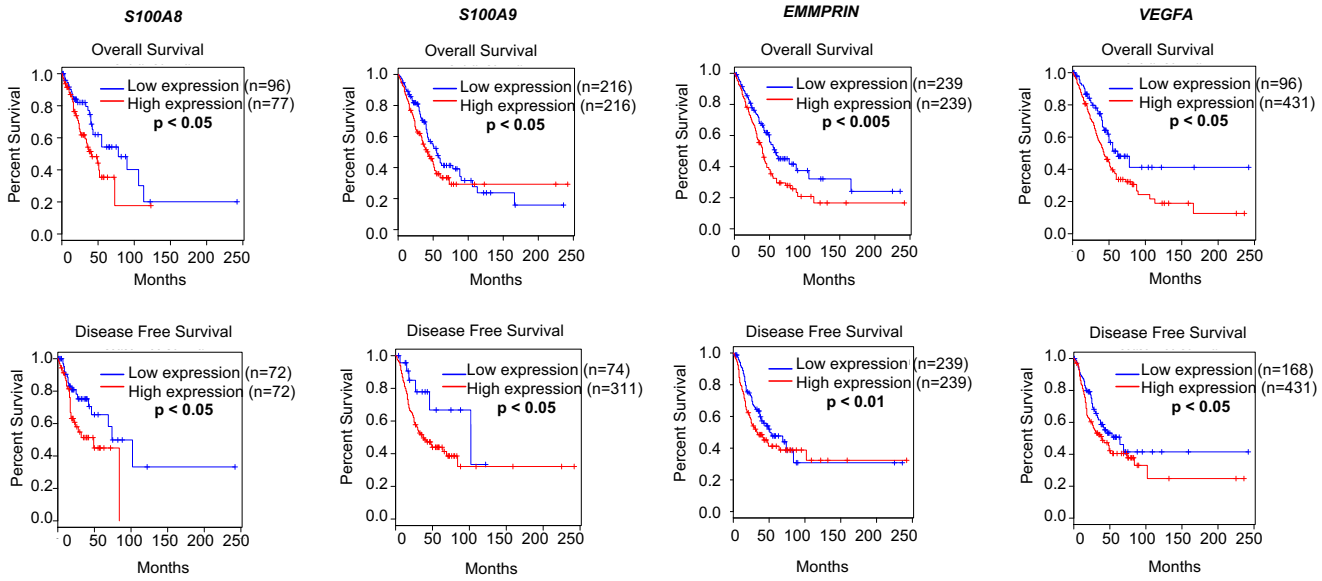

(B)

Lung squamous cell carcinoma

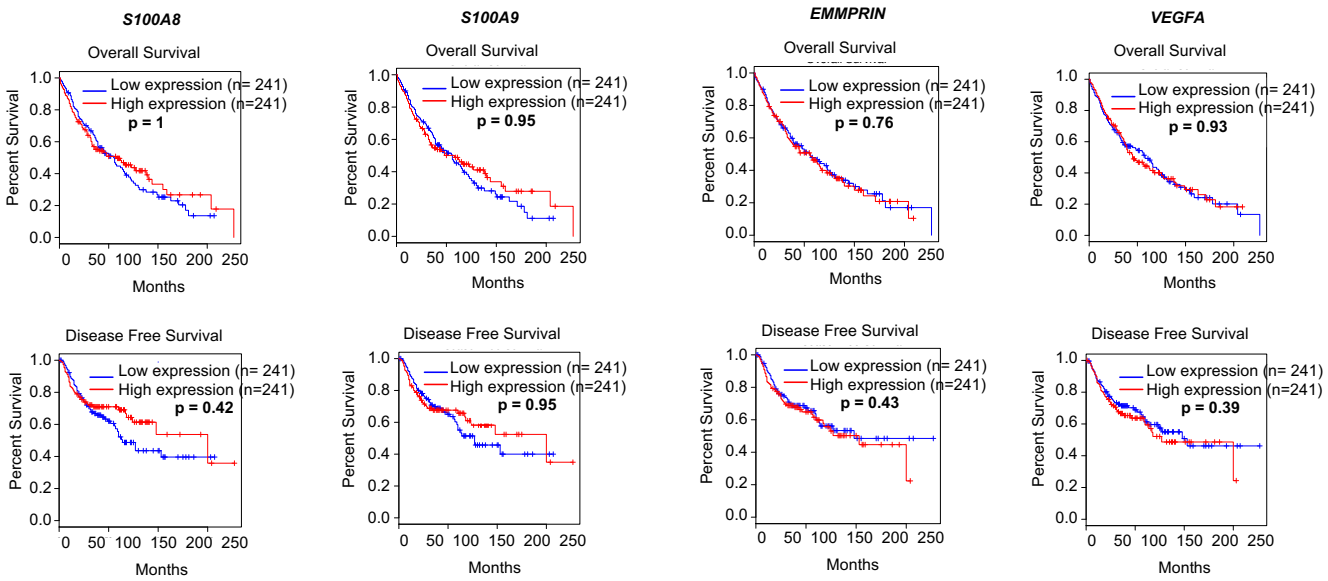

328 **Figure S7. The clinical impact of *S100A8, S100A9, EMMPRIN,* or *VEGFA* expressions in**
329 **lung cancer patients.**
330 A, Overall survival (OS) and disease-free survival (DFS) of patients with lung adenocarcinoma
331 whose tumors show indicated *S100A8, S100A9, EMMPRIN,* or *VEGFA* expression. A log-rank
332 test was applied for statistical analysis.
333 B, OS and DFS comparable to that described in (A) but performed with patients with lung
334 squamous cell carcinoma. A log-rank test was applied for statistical analysis.
335
336

337 **SUPPLEMENTARY TABLES**

338 **Table S1. The top 5 markers highly expressed in clusters of CD45 cells.**

No.	Cluster	gene	p_val	avg_logFC	pct.1	pct.2	p_val_adj
1	GMD1	*S100a9*	0	3.6619474	1	0.61	0
2	GMD1	*S100a8*	0	3.6008872	0.988	0.559	0
3	GMD1	*Gm5483*	0	3.1815544	0.906	0.213	0
4	GMD1	*Retnlg*	7.50E-279	3.0239987	0.873	0.177	1.50E-275
5	GMD1	*Stfa2l1*	4.36E-117	2.809631	0.728	0.194	8.72E-114
6	GMD2	*S100a9*	1.68E-41	1.1820433	1	0.649	3.36E-38
7	GMD2	*S100a8*	2.66E-41	1.132321	1	0.601	5.31E-38
8	GMD2	*Hdc*	2.69E-39	0.8292277	0.989	0.476	5.39E-36
9	GMD2	*G0s2*	1.79E-33	0.9718507	0.819	0.3	3.57E-30
10	GMD2	*Cxcr2*	2.19E-33	0.8683871	0.851	0.326	4.38E-30
51	GMD3	*Cald1*	9.55E-86	2.7566731	0.969	0.259	1.91E-82
52	GMD3	*Gm26917*	2.27E-66	2.9794049	0.962	0.751	4.54E-63
53	GMD3	*Dst*	8.99E-64	2.4593517	0.931	0.555	1.80E-60
54	GMD3	*Hmga2*	3.62E-54	2.2739668	0.838	0.183	7.24E-51
55	GMD3	*Gm26870*	1.84E-10	2.6159146	0.654	0.334	3.69E-07
11	MMD1	*Gngt2*	2.33E-158	1.4121712	0.968	0.72	4.66E-155
12	MMD1	*Adgre5*	1.28E-122	1.0891883	0.839	0.383	2.55E-119
13	MMD1	*Hp*	7.89E-114	1.3351314	0.911	0.603	1.58E-110
14	MMD1	*Chil3*	2.13E-56	1.2319696	0.797	0.553	4.27E-53
15	MMD1	*Fn1*	1.52E-43	1.1886725	0.752	0.597	3.03E-40
16	MMD2	*Vcan*	8.74E-279	1.2098835	0.995	0.829	1.75E-275

17	MMD2	*Itga1*	3.71E-190	0.8937151	0.899	0.664	7.42E-187
18	MMD2	*Fn1*	4.64E-173	0.9650175	0.879	0.571	9.28E-170
19	MMD2	*Chil3*	5.73E-172	1.4652862	0.848	0.53	1.15E-168
20	MMD2	*Dmkn*	6.72E-159	1.0441625	0.824	0.549	1.34E-155
21	MMD3	*Ndrg1*	3.58E-175	1.1753423	0.946	0.795	7.15E-172
22	MMD3	*Hspa1a*	1.08E-138	1.7998893	0.859	0.625	2.16E-135
23	MMD3	*Hsp90aa1*	3.42E-119	1.263954	0.991	0.972	6.85E-116
24	MMD3	*Mt1*	2.32E-115	1.272976	0.949	0.845	4.64E-112
25	MMD3	*Hspa1b*	1.71E-112	1.7265782	0.781	0.516	3.43E-109
26	MMD4	*Mx1*	2.46E-271	1.5392613	0.949	0.637	4.92E-268
27	MMD4	*Ifit3*	3.84E-270	1.6833242	0.962	0.625	7.68E-267
28	MMD4	*Ifit2*	1.06E-248	1.6938069	0.924	0.607	2.12E-245
29	MMD4	*Rsad2*	4.58E-217	1.6653647	0.971	0.763	9.15E-214
30	MMD4	*Cxcl10*	9.14E-145	1.6644475	0.873	0.692	1.83E-141
31	MMD5	*Hmox1*	8.66E-222	1.2093445	0.989	0.901	1.73E-218
32	MMD5	*Prdx1*	1.88E-195	1.2748755	0.994	0.975	3.76E-192
33	MMD5	*Pf4*	7.99E-195	1.5547752	0.889	0.627	1.60E-191
34	MMD5	*Arg1*	1.72E-177	1.605917	0.806	0.569	3.44E-174
35	MMD5	*Ppbp*	1.37E-27	1.3871295	0.37	0.29	2.75E-24
36	TAM1	*C1qa*	4.44E-163	1.1936733	0.853	0.547	8.88E-160
37	TAM1	*C1qc*	1.24E-157	1.0529179	0.856	0.579	2.48E-154
38	TAM1	*C1qb*	4.16E-153	1.147579	0.888	0.708	8.32E-150
39	TAM1	*Ccl7*	2.38E-120	0.9833242	0.864	0.581	4.75E-117
40	TAM1	*Cxcl9*	3.70E-71	1.2126565	0.712	0.568	7.40E-68

41	TAM2	*C1qc*	1.88E-211	1.7674086	0.972	0.587	3.76E-208
42	TAM2	*C1qa*	2.69E-203	1.8822504	0.954	0.558	5.38E-200
43	TAM2	*Cbr2*	5.43E-201	1.5082011	0.871	0.241	1.09E-197
44	TAM2	*C1qb*	1.35E-195	1.6715207	0.978	0.712	2.70E-192
45	TAM2	*Ccl8*	5.33E-171	2.4783197	0.926	0.5	1.07E-167
46	TAM3	*Gm42418*	3.76E-108	1.9809251	1	1	7.52E-105
47	TAM3	*AY036118*	3.07E-63	1.4226547	0.918	0.946	6.14E-60
48	TAM3	*Acp5*	9.93E-10	1.0909412	0.326	0.242	1.99E-06
49	TAM3	*Hbb-bt*	3.50E-08	1.8543822	0.345	0.057	7.00E-05
50	TAM3	*Gm26917*	5.74E-06	1.5556694	0.715	0.757	0.01147014
56	TAM4	*Cpa3*	3.71E-34	2.4811262	0.407	0.051	7.41E-31
57	TAM4	*Top2a*	4.41E-24	2.12114	0.847	0.306	8.81E-21
58	TAM4	*Hist1h2ae*	7.80E-15	2.2044307	0.78	0.415	1.56E-11
59	TAM4	*Tpsb2*	5.62E-14	2.1689507	0.322	0.072	1.12E-10
60	TAM4	*Mcpt4*	0.0002674	2.8145358	0.339	0.086	0.53485904
61	DC1	*H2-Eb1*	1.83E-134	2.838175	1	0.574	3.66E-131
62	DC1	*H2-Aa*	2.17E-132	2.6786995	1	0.643	4.34E-129
63	DC1	*H2-Ab1*	5.38E-130	2.6663118	1	0.75	1.08E-126
64	DC1	*Cd74*	1.08E-127	2.1679369	1	0.828	2.15E-124
65	DC1	*Ifitm1*	3.93E-84	1.9601846	0.972	0.821	7.87E-81
66	DC2	*Ccr7*	3.35E-57	3.63565	1	0.273	6.70E-54
67	DC2	*Fscn1*	3.99E-56	3.0575661	0.952	0.155	7.99E-53
68	DC2	*Serpinb6b*	9.14E-55	3.1305203	0.984	0.275	1.83E-51
69	DC2	*Tbc1d4*	1.88E-52	3.4405529	1	0.275	3.77E-49

70	DC2	*Ccl5*	2.97E-41	3.3221448	0.984	0.446	5.93E-38
71	T	*Cd3g*	1.11E-278	2.8989607	0.987	0.138	2.22E-275
72	T	*Trbc2*	4.62E-268	3.1458226	0.987	0.227	9.24E-265
73	T	*Nkg7*	6.83E-216	3.2795426	0.97	0.326	1.37E-212
74	T	*Gzmb*	1.48E-184	3.0430756	0.911	0.302	2.96E-181
75	T	*Ccl5*	2.01E-136	2.8544928	0.897	0.43	4.01E-133
76	B	*Cd79a*	1.31E-81	2.7842508	0.909	0.035	2.63E-78
77	B	*Iglc3*	6.37E-50	2.5966944	0.909	0.086	1.27E-46
78	B	*Ebf1*	3.63E-47	2.8263811	0.955	0.095	7.26E-44
79	B	*Igkc*	4.59E-35	4.5551395	1	0.133	9.19E-32
80	B	*Ighm*	3.67E-17	2.7625069	1	0.489	7.34E-14

Table S2. The top 20 enrichment pathways in each cluster of Cd45+cells based on scRNA-seq.

CLUSTER	GO	Description	LogP	Enrichment	Z-score
GMD1	R-MMU-6799990	Metal sequestration by antimicrobial proteins	-4.3	32	9.6
GMD1	GO:0050786	RAGE receptor binding	-6.1	24	11
GMD1	GO:0005031	tumor necrosis factor-activated receptor activity	-5	24	9.6
GMD1	GO:1904683	regulation of metalloendopeptidase activity	-3.6	21	7.7

GMD1	GO:0002374	cytokine secretion involved in immune response	-3.6	21	7.7
GMD1	GO:0070339	response to bacterial lipopeptide	-3.6	21	7.7
GMD1	GO:0035662	Toll-like receptor 4 binding	-3.6	21	7.7
GMD1	GO:1905049	negative regulation of metallopeptidase activity	-3.6	21	7.7
GMD1	GO:0071221	cellular response to bacterial lipopeptide	-3.6	21	7.7
GMD1	GO:0071220	cellular response to bacterial lipoprotein	-3.6	21	7.7
GMD1	GO:0070163	regulation of adiponectin secretion	-3.6	21	7.7
GMD1	GO:2000321	positive regulation of T-helper 17 cell differentiation	-3.6	21	7.7
GMD1	GO:0070162	adiponectin secretion	-3.6	21	7.7
GMD1	GO:0005035	death receptor activity	-4.5	19	8.3
GMD1	GO:2000562	negative regulation of CD4-positive, alpha-beta T cell proliferation	-4.5	19	8.3
GMD1	GO:0004908	interleukin-1 receptor activity	-3.4	18	7.1
GMD1	GO:0060613	fat pad development	-3.4	18	7.1
GMD1	GO:0008443	phosphofructokinase activity	-3.4	18	7.1
GMD1	GO:0033029	regulation of neutrophil apoptotic process	-4.3	17	7.9
GMD1	GO:0032493	response to bacterial lipoprotein	-3.2	16	6.6
GMD2	R-MMU-6799990	Metal sequestration by antimicrobial proteins	-6.8	2.10E+02	25
GMD2	GO:0035325	Toll-like receptor binding	-4.7	57	13

GMD2	R-MMU-5686938	Regulation of TLR by endogenous ligand	-4.6	50	12
GMD2	GO:0002523	leukocyte migration involved in inflammatory response	-4.1	36	10
GMD2	R-MMU-8956319	Nucleobase catabolism	-3.6	25	8.4
GMD2	GO:0030593	neutrophil chemotaxis	-5.9	17	9.6
GMD2	GO:0071621	granulocyte chemotaxis	-6.5	16	9.9
GMD2	ko04657	IL-17 signaling pathway	-4.8	16	8.3
GMD2	mmu04657	IL-17 signaling pathway	-4.8	16	8.3
GMD2	R-MMU-6803157	Antimicrobial peptides	-4.7	15	8.2
GMD2	ko04640	Hematopoietic cell lineage	-4.7	15	8.1
GMD2	GO:0034109	homotypic cell-cell adhesion	-3.8	15	7.3
GMD2	GO:0071675	regulation of mononuclear cell migration	-3	15	6.4
GMD2	GO:0071622	regulation of granulocyte chemotaxis	-3	15	6.3
GMD2	GO:1990266	neutrophil migration	-5.3	14	8.5
GMD2	mmu04640	Hematopoietic cell lineage	-4.6	14	7.8
GMD2	GO:1903036	positive regulation of response to wounding	-3.7	14	6.9
GMD2	GO:0016209	antioxidant activity	-3.7	14	6.9
GMD2	GO:0061912	selective autophagy	-2.9	14	6
GMD2	GO:0002833	positive regulation of response to biotic stimulus	-2.9	14	6

GMD3	GO:0005588	collagen type V trimer	-4.1	27	8.7
GMD3	R-MMU-6799990	Metal sequestration by antimicrobial proteins	-4.1	27	8.7
GMD3	GO:0007525	somatic muscle development	-4.1	27	8.7
GMD3	GO:0035061	interchromatin granule	-4.1	27	8.7
GMD3	GO:0051256	mitotic spindle midzone assembly	-5	24	9.4
GMD3	CORUM:3029	Drosha complex	-6	22	10
GMD3	GO:0070934	CRD-mediated mRNA stabilization	-3.7	21	7.7
GMD3	GO:0000395	mRNA 5'-splice site recognition	-3.7	21	7.7
GMD3	GO:0097198	histone H3-K36 trimethylation	-3.7	21	7.7
GMD3	GO:0051255	spindle midzone assembly	-5.7	20	9.6
GMD3	GO:0000022	mitotic spindle elongation	-4.7	20	8.7
GMD3	GO:0042382	paraspeckles	-4.7	20	8.7
GMD3	GO:0051231	spindle elongation	-4.4	18	8.1
GMD3	GO:0021825	substrate-dependent cerebral cortex tangential migration	-3.4	18	7
GMD3	GO:0000912	assembly of actomyosin apparatus involved in cytokinesis	-3.4	18	7
GMD3	GO:0050733	RS domain binding	-3.4	18	7
GMD3	GO:0000915	actomyosin contractile ring assembly	-3.4	18	7
GMD3	GO:0098961	dendritic transport of ribonucleoprotein complex	-3.4	18	7
GMD3	GO:0070937	CRD-mediated mRNA stability complex	-3.4	18	7

GMD3	GO:0098963	dendritic transport of messenger ribonucleoprotein complex	-3.4	18	7
MMD1	GO:0071593	lymphocyte aggregation	-4.1	31	9.4
MMD1	GO:0004563	beta-N-acetylhexosaminidase activity	-4.1	31	9.4
MMD1	GO:0071499	cellular response to laminar fluid shear stress	-4.1	31	9.4
MMD1	GO:0001740	Barr body	-4.1	31	9.4
MMD1	GO:0140031	phosphorylation-dependent protein binding	-4.1	31	9.4
MMD1	GO:0034616	response to laminar fluid shear stress	-3.8	26	8.6
MMD1	GO:0050861	positive regulation of B cell receptor signaling pathway	-3.8	26	8.6
MMD1	GO:0060369	positive regulation of Fc receptor mediated stimulatory signaling pathway	-3.8	26	8.6
MMD1	GO:0010727	negative regulation of hydrogen peroxide metabolic process	-3.8	26	8.6
MMD1	mmu_M00146	NADH dehydrogenase (ubiquinone) 1 alpha subcomplex	-6.9	23	11
MMD1	M00146	NADH dehydrogenase (ubiquinone) 1 alpha subcomplex	-6.9	23	11
MMD1	R-MMU-5621480	Dectin-2 family	-3.6	23	8
MMD1	GO:0032667	regulation of interleukin-23 production	-3.6	23	8
MMD1	GO:0006685	sphingomyelin catabolic process	-3.6	23	8

MMD1	GO:0071541	eukaryotic translation initiation factor 3 complex, eIF3m	-3.6	23	8
MMD1	R-MMU-1236973	Cross-presentation of particulate exogenous antigens (phagosomes)	-3.6	23	8
MMD1	GO:0032627	interleukin-23 production	-3.6	23	8
MMD1	GO:0016479	negative regulation of transcription by RNA polymerase I	-3.6	23	8
MMD1	GO:0038096	Fc-gamma receptor signaling pathway involved in phagocytosis	-3.5	20	7.5
MMD1	GO:0010728	regulation of hydrogen peroxide biosynthetic process	-3.5	20	7.5
MMD2	mmu_M00095	C5 isoprenoid biosynthesis, mevalonate pathway	-6.1	50	14
MMD2	M00095	C5 isoprenoid biosynthesis, mevalonate pathway	-6.1	50	14
MMD2	GO:1900222	negative regulation of amyloid-beta clearance	-4.5	45	11
MMD2	R-MMU-191273	Cholesterol biosynthesis	-11	42	18
MMD2	GO:0008250	oligosaccharyltransferase complex	-5.7	42	13
MMD2	GO:0034663	endoplasmic reticulum chaperone complex	-4.1	34	9.8
MMD2	CORUM:538	Cytochrome c oxidase, mitochondrial	-4.1	34	9.8
MMD2	R-MMU-75205	Dissolution of Fibrin Clot	-4.1	34	9.8
MMD2	ko00900	Terpenoid backbone biosynthesis	-6.2	30	12

MMD2	GO:0006614	SRP-dependent cotranslational protein targeting to membrane	-5.1	30	11
MMD2	GO:0006613	cotranslational protein targeting to membrane	-5	29	10
MMD2	GO:0044548	S100 protein binding	-3.9	29	9.1
MMD2	mmu00900	Terpenoid backbone biosynthesis	-6.1	28	12
MMD2	GO:0015002	heme-copper terminal oxidase activity	-4.7	25	9.6
MMD2	GO:0004129	cytochrome-c oxidase activity	-4.7	25	9.6
MMD2	GO:0016676	oxidoreductase activity, acting on a heme group of donors, oxygen as acceptor	-4.7	25	9.6
MMD2	GO:0016675	oxidoreductase activity, acting on a heme group of donors	-4.7	24	9.4
MMD2	GO:1900221	regulation of amyloid-beta clearance	-3.6	24	8.2
MMD2	GO:0016126	sterol biosynthetic process	-9.6	22	14
MMD2	GO:0006695	cholesterol biosynthetic process	-8.6	22	13
MMD3	GO:0055131	C3HC4-type RING finger domain binding	-5	57	13
MMD3	GO:0032557	pyrimidine ribonucleotide binding	-5	57	13
MMD3	GO:1905323	telomerase holoenzyme complex assembly	-4.7	48	12
MMD3	R-MMU-3371568	Attenuation phase	-8.7	44	16
MMD3	GO:0097201	negative regulation of transcription from RNA polymerase II promoter in response to stress	-6.8	37	13
MMD3	GO:0031545	peptidyl-proline 4-dioxygenase activity	-4.2	36	10

MMD3	GO:0018401	peptidyl-proline hydroxylation to 4-hydroxy-L-proline	-5.4	35	12
MMD3	GO:0019471	4-hydroxyproline metabolic process	-5.3	32	11
MMD3	CORUM:414	(ER)-localized multiprotein complex, in absence of Ig heavy chains	-4	32	9.5
MMD3	GO:0060426	lung vasculature development	-4	32	9.5
MMD3	GO:0051085	chaperone cofactor-dependent protein refolding	-11	29	16
MMD3	M00002	Glycolysis, core module involving three-carbon compounds	-5.1	29	11
MMD3	mmu_M00002	Glycolysis, core module involving three-carbon compounds	-5.1	29	11
MMD3	GO:0015911	plasma membrane long-chain fatty acid transport	-3.9	29	9
MMD3	GO:1903748	negative regulation of establishment of protein localization to mitochondrion	-3.9	29	9
MMD3	CORUM:413	(ER)-localized multiprotein complex, Ig heavy chains associated	-3.9	29	9
MMD3	GO:1902001	fatty acid transmembrane transport	-3.9	29	9
MMD3	GO:0036462	TRAIL-activated apoptotic signaling pathway	-3.9	29	9
MMD3	GO:0042026	protein refolding	-6	27	11
MMD3	GO:0019511	peptidyl-proline hydroxylation	-5	27	10
MMD4	GO:0030430	host cell cytoplasm	-9.5	52	17
MMD4	GO:0033655	host cell cytoplasm part	-9.5	52	17

MMD4	GO:0020003	symbiont-containing vacuole	-9.5	52	17
MMD4	GO:0043656	intracellular region of host	-9.5	52	17
MMD4	GO:0033646	host intracellular part	-9.5	52	17
MMD4	GO:0020005	symbiont-containing vacuole membrane	-7.8	49	15
MMD4	GO:0033643	host cell part	-9.1	47	17
MMD4	GO:1990111	spermatoproteasome complex	-4.7	47	12
MMD4	GO:0060335	positive regulation of interferon-gamma-mediated signaling pathway	-6.1	45	13
MMD4	GO:0060332	positive regulation of response to interferon-gamma	-6.1	45	13
MMD4	GO:0065010	extracellular membrane-bounded organelle	-8.8	43	16
MMD4	GO:0043657	host cell	-8.5	39	15
MMD4	GO:0018995	host	-8.5	39	15
MMD4	GO:0097199	cysteine-type endopeptidase activity involved in apoptotic signaling pathway	-5.8	39	12
MMD4	GO:0035458	cellular response to interferon-beta	-29	37	28
MMD4	GO:0035456	response to interferon-beta	-32	34	28
MMD4	GO:0060333	interferon-gamma-mediated signaling pathway	-12	34	17
MMD4	GO:0039530	MDA-5 signaling pathway	-4.2	34	9.8
MMD4	GO:0042270	protection from natural killer cell mediated cytotoxicity	-4.2	34	9.8
MMD4	GO:0032819	positive regulation of natural killer cell proliferation	-4.2	34	9.8

MMD5	GO:1990379	lipid transport across blood brain barrier	-5.2	71	14
MMD5	GO:1900223	positive regulation of amyloid-beta clearance	-4.9	61	13
MMD5	GO:0045236	CXCR chemokine receptor binding	-7.3	47	15
MMD5	GO:0044754	autolysosome	-5.9	47	14
MMD5	GO:0002604	regulation of dendritic cell antigen processing and presentation	-4.6	47	12
MMD5	GO:0005767	secondary lysosome	-7.2	44	15
MMD5	GO:0033700	phospholipid efflux	-4.3	39	11
MMD5	GO:0008035	high-density lipoprotein particle binding	-4.3	39	11
MMD5	GO:0002468	dendritic cell antigen processing and presentation	-4.3	39	11
MMD5	GO:0030169	low-density lipoprotein particle binding	-6.6	35	13
MMD5	GO:2000343	positive regulation of chemokine (C-X-C motif) ligand 2 production	-4.1	35	10
MMD5	GO:0006750	glutathione biosynthetic process	-4.1	35	10
MMD5	GO:1900221	regulation of amyloid-beta clearance	-5.3	33	11
MMD5	R-MMU-8964038	LDL clearance	-5.3	33	11
MMD5	GO:0010744	positive regulation of macrophage derived foam cell differentiation	-4	33	9.6
MMD5	mmu_M00002	Glycolysis, core module involving three-carbon compounds	-4	33	9.6
MMD5	GO:0034362	low-density lipoprotein particle	-4	33	9.6

MMD5	M00002	Glycolysis, core module involving three-carbon compounds	-4	33	9.6
MMD5	GO:0071813	lipoprotein particle binding	-8.8	32	15
MMD5	GO:0071814	protein-lipid complex binding	-8.8	32	15
TAM1	GO:1902566	regulation of eosinophil activation	-5.6	84	16
TAM1	GO:0042613	MHC class II protein complex	-10	74	21
TAM1	GO:0031727	CCR2 chemokine receptor binding	-5.2	67	14
TAM1	GO:0019886	antigen processing and presentation of exogenous peptide antigen via MHC class II	-12	56	21
TAM1	GO:0023026	MHC class II protein complex binding	-4.9	56	13
TAM1	GO:0043307	eosinophil activation	-4.9	56	13
TAM1	R-MMU-173623	Classical antibody-mediated complement activation	-4.9	56	13
TAM1	GO:0098883	synapse pruning	-6.1	50	14
TAM1	GO:0002495	antigen processing and presentation of peptide antigen via MHC class II	-13	48	20
TAM1	GO:1900223	positive regulation of amyloid-beta clearance	-4.6	48	12
TAM1	CORUM:51	CCT complex (chaperonin containing TCP1 complex)	-4.6	48	12
TAM1	CORUM:132	CCT complex (chaperonin containing TCP1 complex)	-4.6	48	12
TAM1	CORUM:52	CCT complex (chaperonin containing TCP1 complex)	-4.6	48	12

TAM1	GO:0002478	antigen processing and presentation of exogenous peptide antigen	-16	46	22
TAM1	GO:0002504	antigen processing and presentation of peptide or polysaccharide antigen via MHC class II	-13	46	20
TAM1	GO:0042611	MHC protein complex	-13	44	19
TAM1	CORUM:3072	CCT complex (chaperonin containing TCP1 complex), testis specific	-4.4	42	11
TAM1	GO:0019884	antigen processing and presentation of exogenous antigen	-14	36	19
TAM1	GO:1903977	positive regulation of glial cell migration	-5.4	34	11
TAM1	GO:1904851	positive regulation of establishment of protein localization to telomere	-4.1	34	9.8
TAM2	GO:0046149	pigment catabolic process	-5.1	58	13
TAM2	GO:0006787	porphyrin-containing compound catabolic process	-5.1	58	13
TAM2	GO:0150062	complement-mediated synapse pruning	-5.1	58	13
TAM2	GO:0042167	heme catabolic process	-5.1	58	13
TAM2	GO:1990379	lipid transport across blood brain barrier	-6.4	51	14
TAM2	GO:0033015	tetrapyrrole catabolic process	-4.7	46	12
TAM2	GO:0031727	CCR2 chemokine receptor binding	-4.7	46	12
TAM2	GO:0031904	endosome lumen	-4.7	46	12
TAM2	GO:0098883	synapse pruning	-7.4	43	14

TAM2	R-MMU-173623	Classical antibody-mediated complement activation	-4.4	38	11
TAM2	GO:0032489	regulation of Cdc42 protein signal transduction	-4.4	38	11
TAM2	R-MMU-8866427	VLDLR internalisation and degradation	-6.8	35	13
TAM2	R-MMU-190873	Gap junction degradation	-5.5	34	11
TAM2	R-MMU-196025	Formation of annular gap junctions	-5.5	34	11
TAM2	GO:1900223	positive regulation of amyloid-beta clearance	-4.1	33	9.7
TAM2	GO:0010886	positive regulation of cholesterol storage	-4.1	33	9.7
TAM2	GO:0110096	cellular response to aldehyde	-5.3	31	11
TAM2	R-MMU-177504	Retrograde neurotrophin signalling	-5.3	31	11
TAM2	GO:0030132	clathrin coat of coated pit	-8.8	30	14
TAM2	GO:1904350	regulation of protein catabolic process in the vacuole	-3.9	29	9
TAM3	R-MMU-5653656	Vesicle-mediated transport	-2.3	8.3	4.5
TAM3	GO:0031347	regulation of defense response	-2.1	7	4
TAM4	GO:0031262	Ndc80 complex	-6.6	45	13
TAM4	GO:0000942	condensed nuclear chromosome outer kinetochore	-6.6	45	13

TAM4	CORUM:1122	Smcb-Smcd-PW29 complex	-5	45	11
TAM4	GO:0032133	chromosome passenger complex	-7.5	37	13
TAM4	GO:0051256	mitotic spindle midzone assembly	-7.5	37	13
TAM4	R-MMU-2980767	Activation of NIMA Kinases NEK9, NEK6, NEK7	-5.9	36	12
TAM4	CORUM:47	DNA polymerase alpha-primase complex	-4.4	34	9.9
TAM4	M00261	DNA polymerase alpha / primase complex	-4.4	34	9.9
TAM4	GO:1905340	regulation of protein localization to kinetochore	-4.4	34	9.9
TAM4	GO:0000799	nuclear condensin complex	-4.4	34	9.9
TAM4	GO:1905342	positive regulation of protein localization to kinetochore	-4.4	34	9.9
TAM4	mmu_M00261	DNA polymerase alpha / primase complex	-4.4	34	9.9
TAM4	CORUM:1110	DNA polymerase alpha-primase complex	-4.4	34	9.9
TAM4	GO:0032564	dATP binding	-4.4	34	9.9
TAM4	GO:0005658	alpha DNA polymerase:primase complex	-4.4	34	9.9
TAM4	GO:0051987	positive regulation of attachment of spindle microtubules to kinetochore	-7	32	12
TAM4	GO:0010032	meiotic chromosome condensation	-7	32	12
TAM4	CORUM:309	RC complex	-7	32	12
TAM4	GO:0000022	mitotic spindle elongation	-7	32	12
TAM4	GO:0000778	condensed nuclear chromosome kinetochore	-16	30	19
DC1	GO:0042613	MHC class II protein complex	-16	59	23

DC1	GO:0023026	MHC class II protein complex binding	-11	59	19
DC1	GO:0023029	MHC class Ib protein binding	-7.1	59	15
DC1	GO:0045338	farnesyl diphosphate metabolic process	-4.7	44	11
DC1	GO:0043435	response to corticotropin-releasing hormone	-4.7	44	11
DC1	GO:2001199	negative regulation of dendritic cell differentiation	-4.7	44	11
DC1	GO:0002584	negative regulation of antigen processing and presentation of peptide antigen	-4.7	44	11
DC1	GO:0071376	cellular response to corticotropin-releasing hormone stimulus	-4.7	44	11
DC1	GO:0023023	MHC protein complex binding	-12	39	17
DC1	GO:1990111	spermatoproteasome complex	-4.3	35	10
DC1	GO:0042611	MHC protein complex	-17	33	20
DC1	GO:0042270	protection from natural killer cell mediated cytotoxicity	-5.6	33	11
DC1	GO:0002583	regulation of antigen processing and presentation of peptide antigen	-5.6	33	11
DC1	GO:0002578	negative regulation of antigen processing and presentation	-5.6	33	11
DC1	GO:0019886	antigen processing and presentation of exogenous peptide antigen via MHC class II	-10	29	15
DC1	CORUM:676	Metallothionein-3 complex	-4	29	9.1

DC1	GO:0002478	antigen processing and presentation of exogenous peptide antigen	-14	26	17
DC1	GO:0002495	antigen processing and presentation of peptide antigen via MHC class II	-11	25	15
DC1	R-MMU-8934593	Regulation of RUNX1 Expression and Activity	-3.8	25	8.4
DC1	GO:2001198	regulation of dendritic cell differentiation	-3.8	25	8.4
DC2	CORUM:6279	p65-IkappaBalpha-beta-arrestin-iNOS complex	-4.4	29	9.2
DC2	GO:0046979	TAP2 binding	-4.4	29	9.2
DC2	GO:0002485	antigen processing and presentation of endogenous peptide antigen via MHC class I via ER pathway, TAP-dependent	-4.4	29	9.2
DC2	R-MMU-8984722	Interleukin-35 Signalling	-9.4	26	13
DC2	GO:0046978	TAP1 binding	-3.8	22	7.9
DC2	GO:2001199	negative regulation of dendritic cell differentiation	-3.8	22	7.9
DC2	R-MMU-9020591	Interleukin-12 signaling	-6.1	21	9.9
DC2	GO:0046977	TAP binding	-9.1	20	12
DC2	GO:0062061	TAP complex binding	-6.9	20	10
DC2	CORUM:2836	Profilin 1 complex	-4.7	20	8.6
DC2	GO:0042824	MHC class I peptide loading complex	-9.6	18	12
DC2	GO:0005131	growth hormone receptor binding	-3.4	18	7

DC2	GO:1902951	negative regulation of dendritic spine maintenance	-3.4	18	7
DC2	GO:0031904	endosome lumen	-3.4	18	7
DC2	GO:0060397	JAK-STAT cascade involved in growth hormone signaling pathway	-3.4	18	7
DC2	R-MMU-9020958	Interleukin-21 signaling	-4.4	17	7.9
DC2	CORUM:5742	Multicomponent signaling complex, anti-CD40 stimulated,(Birc2, Birc3, Cd40, Ikbkg, Map3k1, Traf2, Ube2n)	-4.4	17	7.9
DC2	GO:0042270	protection from natural killer cell mediated cytotoxicity	-4.4	17	7.9
DC2	R-MMU-1810476	RIP-mediated NFkB activation via ZBP1	-6.2	16	9.4
DC2	GO:0042610	CD8 receptor binding	-6.2	16	9.4
T	M00285	MCM complex	-7.4	17	9.8
T	mmu_M00285	MCM complex	-7.4	17	9.8
T	CORUM:122	MCM complex	-7.4	17	9.8
T	R-MMU-156842	Eukaryotic Translation Elongation	-6.2	17	9
T	GO:0000275	mitochondrial proton-transporting ATP synthase complex, catalytic core F(1)	-6.2	17	9
T	GO:0023024	MHC class I protein complex binding	-6.2	17	9
T	CORUM:5310	Cd3d-Cd3g-Cd3e-Cd247 complex	-4.9	17	8

T	GO:0032831	positive regulation of CD4-positive, CD25-positive, alpha-beta regulatory T cell differentiation	-3.7	17	7
T	GO:0099040	ceramide translocation	-3.7	17	7
T	CORUM:2874	Slam-SAP-FynT complex	-3.7	17	7
T	GO:1990518	single-stranded DNA-dependent ATP-dependent 3'-5' DNA helicase activity	-3.7	17	7
T	GO:0043140	ATP-dependent 3'-5' DNA helicase activity	-3.7	17	7
T	GO:0099038	ceramide-translocating ATPase activity	-3.7	17	7
T	GO:0019976	interleukin-2 binding	-3.7	17	7
T	CORUM:2568	Slam-SAP-FynT complex	-3.7	17	7
T	R-MMU-202430	Translocation of ZAP-70 to Immunological synapse	-9	15	11
T	GO:1990446	U1 snRNP binding	-7.8	15	9.9
T	GO:0005688	U6 snRNP	-7.8	15	9.9
T	M00397	Lsm 1-7 complex	-6.6	15	9
T	CORUM:132	CCT complex (chaperonin containing TCP1 complex)	-6.6	15	9
B	R-MMU-156842	Eukaryotic Translation Elongation	-7.5	31	12
B	CORUM:161	SWAP complex	-6	31	11
B	GO:0002344	B cell affinity maturation	-4.5	31	9.5
B	GO:0002343	peripheral B cell selection	-4.5	31	9.5

B	GO:0042613	MHC class II protein complex	-11	28	15
B	GO:0019815	B cell receptor complex	-8.1	27	12
B	GO:0023026	MHC class II protein complex binding	-6.7	26	11
B	GO:0035061	interchromatin granule	-3.9	23	8.1
B	GO:1902308	regulation of peptidyl-serine dephosphorylation	-3.5	19	7.2
B	GO:0051025	negative regulation of immunoglobulin secretion	-3.5	19	7.2
B	GO:0002339	B cell selection	-3.5	19	7.2
B	GO:0070087	chromo shadow domain binding	-3.5	19	7.2
B	GO:0035022	positive regulation of Rac protein signal transduction	-3.5	19	7.2
B	R-MMU-5690714	CD22 mediated BCR regulation	-3.5	19	7.2
B	GO:0031618	nuclear pericentric heterochromatin	-5.4	17	8.9
B	GO:1990446	U1 snRNP binding	-4.2	16	7.5
B	GO:0061470	T follicular helper cell differentiation	-3.2	16	6.5
B	GO:0019886	antigen processing and presentation of exogenous peptide antigen via MHC class II	-6.5	14	9.2
B	CORUM:572	PYR complex	-4.7	13	7.5
B	GO:0023023	MHC protein complex binding	-4.7	13	7.5

342

343 **Table S3. FPKM values of S100a8/S100a9 and corresponding receptors.**

Gene name	LLC-in vitro 1	LLC-in vitro 2	LLC-in vitro 3	LLC-in vitro 4	LLC-in vitro 5	LLC-in vivo 1	LLC-in vivo 2	LLC-in vivo 3	LLC-in vivo 4	LLC-in vivo 5
S100a8	0.01	1.07795	0.01	0.47757	0.14327	5.82864	0.79694	1.9622	3.01905	5.20144
S100a9	0.01	0.01	0.01	0.01	0.01	2.96642	0.41995	1.4042	2.03824	4.14339
Tlr4	17.8483	28.6618	16.4358	45.4713	35.9133	7.06859	9.60603	8.8262	9.60366	12.4807
Bsg	216.754	526.04	262.269	568.808	453.189	500.371	287.381	281.49	398.37	328.438
Ager	0.56347	0.11518	0.80036	0.62453	0.28791	0.55943	1.09225	2.553	0.53609	0.69442

Table S4. Top 10 significantly enriched pathways from GO and KEGG enrichment analysis of WTA data of LLC cells.

GO	Description	LogP	Enrichment	Z-score
GO:1901342	regulation of vasculature development	-13	5.4	10
GO:0045765	regulation of angiogenesis	-12	5.6	10
GO:0001568	blood vessel development	-12	3.7	9.1
ko05230	Central carbon metabolism in cancer	-9.8	12	11
ko04668	TNF signaling pathway	-8.1	8.1	9.1
R-MMU-1280215	Cytokine Signaling in Immune system	-5.6	2.9	5.7
GO:0043408	regulation of MAPK cascade	-5.3	2.6	5.3
GO:0070372	regulation of ERK1 and ERK2 cascade	-4.6	3.4	5.3
GO:0001819	positive regulation of cytokine production	-4.5	2.8	5
GO:0001558	regulation of cell growth	-4.4	2.9	4.9

348 **Table S5. Top 10 significantly enriched pathways from GO and KEGG enrichment**

349 **analysis of scRNA-seq data and WTA data of GMD, MMD and TAMs.**

GO	Description	_LogP_CD45scRNAseq	_LogP_mRNAseq-GMD	_LogP_mRNAseq-MMD	_LogP_mRNAseq-TAM
GO:0071347	cellular response to interleukin-1	-3.6292191	-3.6924162	-7.6439643	-3.2133256
GO:1904951	positive regulation of establishment of protein localization	-6.1902007	-3.8007701	-6.7694037	-2.1373743
ko04657	IL-17 signaling pathway	-7.9299785	-3.2933656	-10.99263	-2.8586514
GO:0000165	MAPK cascade	-8.7034568	-2.5237574	-7.7411943	-2.8670897
GO:0097529	myeloid leukocyte migration	-12.53702	-8.6046712	-5.1965013	-3.0926284
GO:0019221	cytokine-mediated signaling pathway	-10.835677	-4.7070109	-9.1717688	-3.8588184
GO:0006954	inflammatory response	-15.606855	-8.4392808	-19.346601	-3.5283674
GO:0050900	leukocyte migration	-16.03232	-8.2135698	-7.0066308	-4.8721725
GO:0050673	epithelial cell proliferation	-4.3945533	-2.1704342	-3.5826776	-2.4066515
GO:0009725	response to hormone	-4.4851442	-2.2287992	-3.0013683	-4.4607612

350

351

352

353 **Table S6. WTA indicated gene expression of MMPs in LLC.**

Gene name	WT78-LLC_R1 (paired) (GE) - RPKM	WT83-LLC_R1 (paired) (GE) - RPKM	WT82-LLC_R1 (paired) (GE) - RPKM	KO79-LLC_R1 (paired) (GE) - RPKM	KO84-LLC_R1 (paired) (GE) - RPKM	KO81-LLC_R1 (paired) (GE) - RPKM
Mmp10	0	0.38141553	0.60154053	2.50124789	0.48660632	0.20807941
Mmp11	2.12912295	1.96690323	2.57126968	2.61113628	2.3356084	2.58605835
Mmp12	0.18677203	0.45622082	0.8489396	3.61938645	0.88802184	0.16670749
Mmp13	0.04767706	0.18428663	0.12492564	0.27497506	0.08089846	0.04468297
Mmp14	36.989615	32.2354347	31.5931334	44.3295353	32.1254212	36.9800087
Mmp15	0	0	0.01459845	0	0.00526391	0.00664557
Mmp16	0.08015144	0	0.00233785	0	0	0.00292667
Mmp17	0	0.0191762	0.00212234	0	0	0.00797065
Mmp19	6.12660585	3.94092793	3.61365111	4.61907934	5.64401149	5.45526013
Mmp1a	0	0.08112618	0.09090917	0.09441807	0.09348388	0.05058057
Mmp1b	0	0.16997866	0.08935928	0.25362607	0.08394471	0.11775371
Mmp2	12.9593779	13.0164556	14.9160004	23.6692744	14.1254292	14.0829473
Mmp20	0	0	0.00414653	0	0.00411168	0.01557272
Mmp21	0	0.02209357	0.0146713	0	0	0
Mmp23	0	0.14313057	0.1188079	0.06150697	0.06597328	0.22012306
Mmp24	0.01973073	0.15253078	0.27696091	0.14338296	0.160072	0.21001234
Mmp25	0	0.00774087	0.0102807	0.03880866	0.0101943	0.02895769
Mmp27	0	0	0.00616726	0	0	0

Mmp28	2.76898363	1.69681401	1.78767165	2.04883088	1.13521096	1.30432822
Mmp3	7.8073106	10.0630246	11.9609379	43.8229848	16.0365158	5.26275702
Mmp7	0	0	0	0.0137642	0	0
Mmp8	0.1051058	0	0	0	0	0
Mmp9	0.63158283	0.31736426	0.45594253	0.19670161	0.30944471	0.26382713

354